Transactions of the Materials Research Society of Japan 29 [2] 421-424 (2004)

TEM and XPS analysis of (Ti,Cr)CN/DLC superhard nanocomposite coatings

Yongqing Fu, [1,2] Sam Zhang [1], Hejun Du [1,2]

[1] School of MPE, Nanyang Technological University, Singapore 639798

[2] Advanced Materials for Micro and Nano Systems Programme, Singapore-MIT Alliance, 4 Engineering Drive 3, Singapore 117576

Fax: 65-67911859, e-mail: myqfu@ntu.edu.sg

Superhard nanocomposite (Ti,Cr)CN/DLC coatings were prepared through co-sputtering of Ti, Cr and graphite targets in an argon/nitrogen atmosphere. Transmission electron microscopy observation revealed that many nano-size TiCrCN crystals (5-12 nm with different orientations and lattice spacings) were embedded in amorphous carbon and/or carbon nitride matrix. The average distance among these nanocrystals was about 10 nm, and the volume percentage of these nano-grains was about 70%. X-ray photoelectron spectroscopy analysis was performed and both surface chemistry and composition evolution with depth for the deposited nanocomposite coatings were characterized.

Key words: Nanocomposite coating, diamond like carbon, nanocrystals, sputtering, superhardness, TEM, XPS

1. INTRODUCTION

Nanocomposite coatings have recently attracted increasing interests because of the possibilities of synthesizing materials with unique physical-chemical properties [1,2]. So far, extensive theoretical and experimental efforts have been made to synthesize and study these nanocomposite coatings with superhardness and high toughness [3,4]. Grain boundary hardening is one of the possibilities to increase coating hardness. However, a new deformation mechanism, grain boundary sliding, dominates the deformation process when the grain size is down to nanometers, causing the significant decrease in coating hardness. Further increase in coating hardness or strength beyond this size limitation can only be achieved if grain boundary sliding is prevented through proper coating design, i.e., by increasing the complexity and strength of grain boundaries in the nanocomposite coatings. This can be realized by optimal design of multiple phases, thus maximizing interfaces and formation of well-defined interfaces with high cohesive strength [5,6]. It is better to use ternary, quarternary or even more systems, with a combination of tough, high strength amorphous matrix to improve toughness and different types of refractory and immiscible metal-nitride nanocrystals to increase grain boundary complexity and strength. One popular design method is to embed nanocrystalline phases in an amorphous matrix [7,8]. Diamond like carbon (DLC), amorphous carbon nitride or other hard amorphous materials have been recognized as the primary candidates for the amorphous matrix, while nano-sized refractory nitrides, such as TiN, CrN, Si_3N_4, AlN, BN, etc. could be used as strengthening phases [9,10]. Following the above design concept, in this study, the nanocomposite TiCrCN/DLC coatings were prepared and their microstructure and chemical bonding were studied. DLC (or amorphous CN_X) acts as hard, tough and lubricating matrix, while nano-particles of TiN, TiC, CrN, TiCN, etc. act as reinforcing crystallites to improve hardness and mechanical properties.

2. EXPERIMENTAL

A multi-target magnetron sputtering system was used to prepare $(TiCr)C_xN_y$/DLC nano-composite coatings. Graphite, Ti and Cr targets were co-sputtered with nitrogen gas flow ratio $[N_2/(N_2+Ar)]$ of 33%. Ar/N_2 gas pressure was 5 mTorr. Ti target power density was optimized as 6.5 W/cm^2 (D.C.), and those of Cr and graphite targets were 4.5 W/cm^2 (D.C.) and 6.5 W/cm^2 (RF), respectively. The substrate-to-target distance was 100 mm. Silicon wafers were used as the substrates, and pre-cleaning of specimens for 5 minutes before deposition was performed with bias power of 100 W. The substrate holder was rotated during the deposition for uniformity. During sputtering, an optimized temperature of 150°C was chosen to promote growth of crystalline phase. The substrate bias power was RF 100 W. Microstructure of the coating was examined using transmission electron microscopy (TEM, JEOL JEM-2000EX). X-ray photoelectron spectroscopy (XPS) analysis was performed on the sample surface using a Kratos-Axis spectrometer with monochromatic Al Kα (1486.71 eV) X-ray radiation. To remove surface contamination layer,

Ar ion bombardment was carried out for 600 seconds using a differential pumping ion gun (Kratos MacroBeam) with an accelerating voltage of 4 keV. Film hardness was evaluated using a nano-indentation tester with a penetrating depth of 100 nm, and the calculation of hardness value was performed automatically using Oliver and Pharr method. Curvature changes of a 4-inch Si wafer before and after film deposition were measured using a Tencor FLX-2908 laser system, from which the film stress was derived.

3. RESULTS AND DISCUSSIONS

3.1 Microstructure

Nano-indentation results show that the film hardness is about 36±2 GPa. Curvature measurement shows that the film stress is about 0.77 GPa. Veprek et al suggested that the real coating hardness should be the value measured with a low film stress (less than 1 GPa) [2]. Since the film stress is 0.77 GPa, it can be concluded that the obtained hardness is the true value, and the film is really superhard.

Fig. 1(a) shows a low-magnification bright-field TEM photo of the deposited films. In an amorphous matrix, many nano-size crystals can be observed with dimensions about 5-12 nm. EDX analysis reveals that the matrix is mainly composed of C and N. Fig. 1(b) shows high-magnification TEM images of these nanocrystals. These crystals have different orientations and lattice spacings, and many crystals show the mottled structure. The crystalline lattices are disrupted by the structural interfaces, mis-oriented and amorphous regions. The average distance between these nanocrystals is about 8 to 10 nm, and the volume percentage of these nano-grains is about 70%. The corresponding selected area electron diffraction pattern shown in Fig. 1(c) confirms the crystalline structure of (Ti,Cr)N nanocrystals. In general, (1 1 1), (2 0 0) and (2 2 0) exhibit the more distinct rings than other diffraction rings. Fig. 1(d) shows the dark-field TEM photos, clearly revealing these nano-size crystals. XRD profile of the film reveals the crystalline structure. There are some broad peaks of (TiCr)CN crystalline phases, corresponding to (1 1 1), (2 0 0) and (2 2 0) peaks, which can strongly support the TEM observation [7].

In brief, TEM observation confirms the realization of DLC based nanocomposite coating design (shown in Fig. 1) through the multi-target sputtering method. Mean crystallite size of 5-12 nm is obtained with entire crystallite surfaces covered with amorphous materials. These features are expected to impede dislocation slip and make plastic deformation more difficult, thus increasing the film hardness.

3.2 XPS analysis

Fig. 2 shows XPS depth profile of the nanocompociste film, showing the elemental composition of the films in term of atomic percentage. The inspection of the profile shows two regions. The first region is close to the surface and characterised by high oxygen and carbon contents, and the dominant signals are from C, O, N, Cr and Ti. The surface oxide and carbon diffusion depth is about 20 nm if calculating using the calibrated etching rate of 3 nm/min. The second region presents the average composition of the bulk film. In the bulk film, oxygen content is quite low. Carbon content also decreases significantly. Nitrogen, chromium and titanium content increases significantly and then remain a stable value.

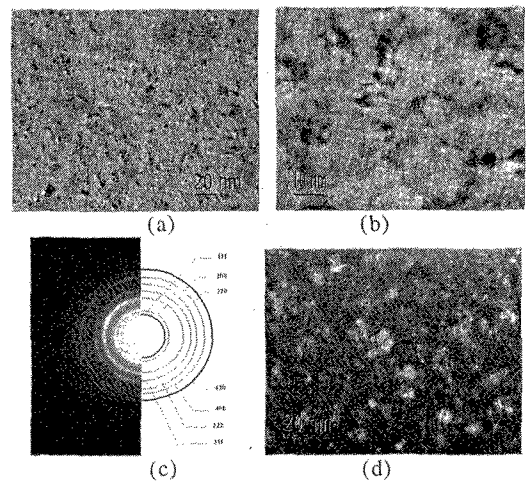

Fig. 1. TEM photo of TiCrCN nanocomposite coating showing nano-size TiCrCN crystals embedded into the amorphous DLC matrix. (a) low magnification image; (b) High magnification; (c) diffraction pattern; (d) dark-field image

Fig. 3(a) shows the Ti 2p core level spectra evolution with depth. Based on the literature values [11], the features at 454.9 eV and 460.8 eV are assigned to TiN (2p ½ and 3/2), and those at 458.8 eV and 464.8 eV to TiO_2. There are two other broad components at about 457.1 eV and 463.5 eV, which can be assigned to Ti-X peak (a combination of substoichiometric TiNx (x<1) and TiOx (or TiNxOy), as well as Ti 2p intrinsic satellite peak [14]). Titanium satellite peaks are commonly observed, and they are loss peaks due to the check-up phenomena related to the screening effect of conduction electrons, or an electronic effect brought by atomic reordering [12]. The Ti 2p1/2 and 3/2 peaks of TiN phase are situated at higher positions compared with 453.8 and 459.9 eV of pure Ti 2p, indicating a charge transfer. The quantitative deconvolution results of relative ratios of TiN, Ti-X and TiO_2 are shown in Fig. 3(b) as a function of sputtering time. On the film surface, TiO_2 peaks and Ti-X peaks are dominant. With the increase of depth, it is reasonable to observe that Ti-O component decreases and Ti-N component increases significantly. Ti-X contents remain large volume (about 30-40 at%) with depth. At film surface,

large amount of Ti-X components can be attributed to sub-stoichionmetric Ti oxides [13]. With the increase of depth, most of oxygen has been sputtered away, and the contribution from sub-stoichiometric TiNx, and satellite components becomes significant. Deep into the film, the TiN and the TiN_X components are the major contributions.

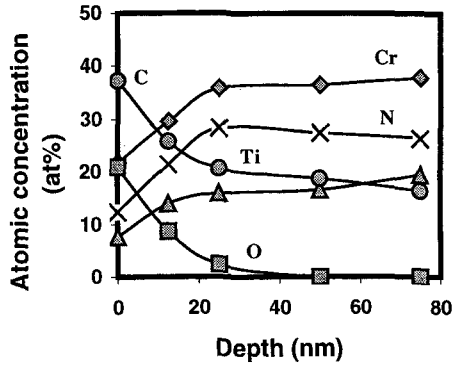

Fig. 2. Atomic concentration changes with depth for the nanocomposite coatings

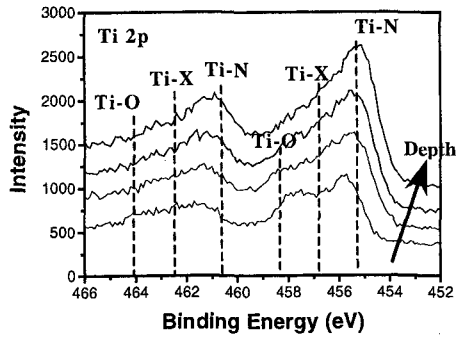

(a) Ti 2p spectrum

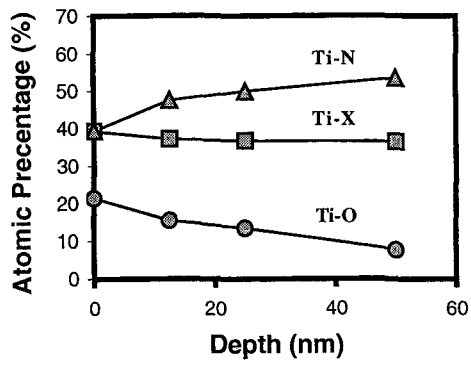

(b). Ti 2p components

Fig. 3. Ti 2p spectrum evolution

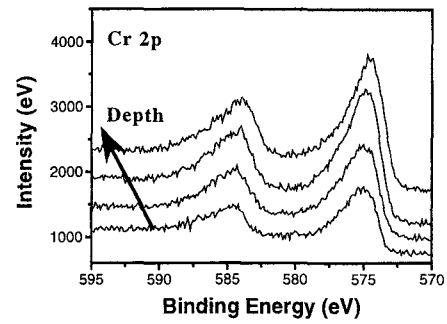

Fig. 4. Evolution of Cr 2p peak with depth for the nanocomposite coatings

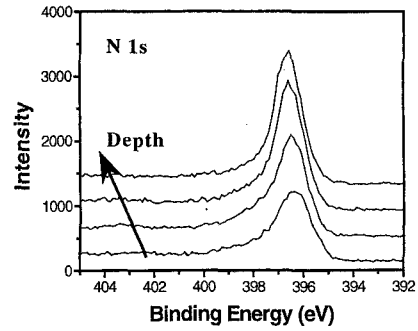

Fig. 5. Evolution of N 1s peak with depth for the nanocomposite coatings

Fig. 4 shows the Cr 2p core level spectra evolution with depth. There is not significant change in Cr 2p spectra vs. depth, and the two main peaks are mainly corresponding to Cr 2p 3/2 and Cr ½ of Cr-N and metallic Cr components. This indicates that some Cr elements do not react with N and maintain a metallic state. A higher binding energy shoulder of Cr 2p 3/2 peak and Cr 2p ½ peak can be observed indicating the formation of a certain amount of Cr(N,O) and oxide species due to air exposure. However, this binding energy shoulder may be attributed to Cr_2N because its binding energy (577.7 eV) is very close to that of Cr(N,O) (577.2) and Cr_2O_3 (578.2 eV). The peaks of Cr_2O_3 are not so apparent.

Fig. 5 shows the evolution of the N 1s spectra as a function of depth. The N1s binding energy values fall in a relatively broad energy range between 396 and 398 eV. Nitrides of Ti and Cr are located in the binding energy between 396 and 397 eV (CrN of 396.5 eV and TiN of 396.7 eV, thus it is difficult to deconvolute). On the film surface, apart from the main features of nitrides, there is one minor component with broad range from 398 to 400 eV, possibly the combination of N-C (398.3 eV, N-C sp^3 bonding

and 399.1 eV N-C sp^2 bonding) and N-O (401 eV).

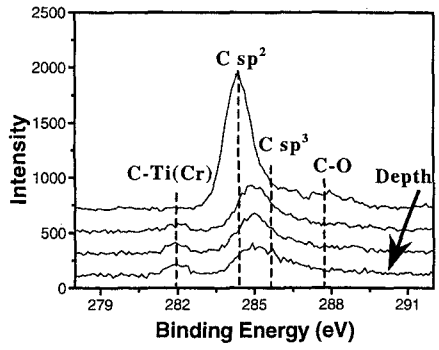

6(a)

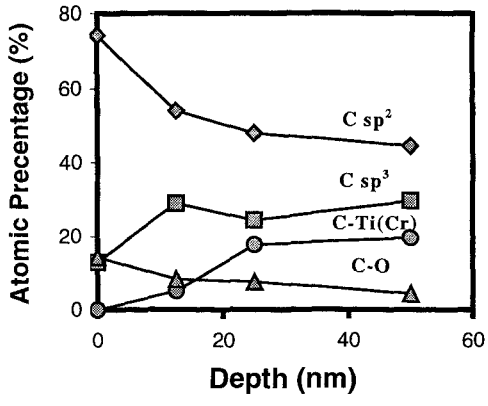

6(b) Atomic concentration changes with depth

Fig. 6. Evolution of C 1s peak with depth for the nanocomposite coatings

Fig. 6(a) shows the evolution of the C 1s spectrum as a function of depth. The C 1s spectrum on the film surface has a main feature at 284.6 eV assigned to adventitious hydrocarbon. A small and broad peak at 288.3 eV is correspondent to C-O bonding. With a short time sputtering using Ar ion beam, the peak at 284.6 eV decreases and C-O bond disappears, indicating that these are from surface contamination. In the bulk film, there is a broad peak between 284.6 eV to 287 eV, which is a combination of 284.7 eV (C-C or C-N sp^2 bonding) and 286.6 eV (C-C or C-N sp^3 bonding). Another main peak at about 282 eV corresponds to C-Ti (or C-Cr) bond. The changes of concentrations of the different bonding structures for C 1s peaks are calculated as a function of etching depth and the results are shown in Fig. 6(b). In the films, there are three main components, C-C (or C-N) sp^2 and sp^3, and TiC, indicating TiCN (or CrCN) crystals are embedded in amorphous carbon or CNx matrix, and this can further confirm TEM observations.

4. CONCLUSIONS

Superhard nanocomposite (Ti,Cr)CN/DLC coatings were prepared through co-sputtering of Ti, Cr and graphite targets in an argon/nitrogen atmosphere. Transmission electron microscopy observation revealed that many nano-size TiCrCN crystals (5-12 nm with different orientations and lattice spacing) were embedded in amorphous carbon and/or carbon nitride matrix. The average distance among these nanocrystals was about 10 nm, and the volume percentage of these nano-grains was about 70%. X-ray photoelectron spectroscopy analysis was performed on film surface using a Kratos AXIS spectrometer with monochromatic Al Kα X-ray radiation. Both surface chemistry and composition evolution with depth for the deposited nanocomposite coatings were characterized.

5. REFERENCES

[1] S. Zhang, D. Sun, Y.Q. Fu, H. J. Du, *Surf. Coat. Technol.*, 167, 113 (2003).
[2] S.Veprek and S.Reiprich, *Thin Solid Films*, 268, 64 (1995).
[3] S.Veprek and A.S.Argon, *Surf. Coat. Technol.*, 146-147, 175 (2001).
[4] J. Musil and H. Hruby, *Thin Solid Films*, 36, 104 (2000).
[5] M.Stuber and V.Schier, *Surf. Coat. Technol.*, 74-75, 833 (1995).
[6] S.Carvalho and L.Rebouta, *Thin Solid Films*, 398-399, 391 (2001).
[7] S. Zhang, Y.Q. Fu, H.J. Du, X. T. Zeng, Y. C. Liu, *Surf. Coat. Technol.*, 162, 42 (2002).
[8] S.Veprek and M.Haussmann: *Surf. Coat. Technol.*, 86-87, 394 (1996).
[9] A.A.Voevodin, J. P. O'Neill, S. V. Prasad, J. S. Zabinski, *J. Vac. Sci. Technol.*, A 17, 986 (1999).
[10] S.Veprek, *J.Vac.Sci.Technol.*, A17, 2401 (1999).
[11] J. Kovac, G. Scarel, M. Sancrotti, et al., *J. Appl. Phys.*, 86, 5566 (1999).
[12] M. Delfino, J. A. Fair, D. Hodul, *J. Appl. Phys.*, 71, 6079 (1992).
[13] I. Strydom and S. Hofmann, *J. Electron. Spectroscopy. Relat. Phenom.*, 56, 85 (1991).
[14] J. Guillot, F. Fabreguette, L. Imhoff, et al, *Appl. Surf. Sci.*, 177, 268 (2001).

(Received October 10, 2003; Accepted March 31, 2004)